RSC Advances

PAPER

View Article Online
View Journal | View Issue

Check for updates

Cite this: *RSC Adv.*, 2018, **8**, 21306

Chemical and thermal properties of VO_2 mechanochemically derived from V_2O_5 by co-milling with paraffin wax†

Chika Takai, [a] Mamoru Senna, *[ab] Satoshi Hoshino, [a] Hadi Razavi-Khosroshahi [a] and Masayoshi Fuji *[a]

A novel mechanochemical reduction process of V_2O_5 to VO_2 was established by milling with paraffin wax (PW, average molecular weight 254–646), serving as a reductant. The reduction progressed with increasing milling time and mass ratio V_2O_5 : PW (MRVP). The mechanochemically derived VO_2 became phase pure after milling for 3 h with an MRVP of 30 : 1 and exhibited a reversible polymorphic transformation between tetragonal and monoclinic phases at around 53–60 °C and 67–79 °C during heating and cooling, respectively. The latent heat was above 20 J g^{-1} in both processes, being superior to those of commercial VO_2. Doping of starting V_2O_5 with Cr, Mo or W at 1 at% in the form of oxide did not increase the latent heat. This is another difference from the conventionally prepared doped VO_2. These anomalous heat storage properties of mechanochemically derived VO_2 were discussed mainly on the basis of X-ray photoelectron spectroscopy $V_{2p3/2}$ peaks combined with ion etching. The observed relatively high heat storage capacity of undoped VO_2 is primarily ascribed to the abundance of V^{4+} ionic states introduced during milling with PW, which were stabilized with simultaneously introduced structural degradation throughout the entire particles. The possible role of a remaining small amount of PW was also discussed.

Received 12th March 2018
Accepted 29th May 2018

DOI: 10.1039/c8ra02159g

rsc.li/rsc-advances

Open Access Article. Published on 11 June 2018. Downloaded on 1/25/2026 10:46:13 PM.
This article is licensed under a Creative Commons Attribution-NonCommercial 3.0 Unported Licence.

Introduction

Vanadium oxides exhibit a series of varying oxidation states, *i.e.* V(v)$_2$O$_5$, V(IV)O$_2$, V(III)$_2$O$_3$ and V(II)O. While that with the highest oxidation state, V_2O_5, is most stable, VO_2 gathers increasing interest due to its various functions, among others, for latent heat storage.[1,2] VO_2 exhibits a reversible polymorphic transformation between monoclinic and tetragonal phases at around 68 °C.[3] This unique Mott transition (MTT) enables energy management or optoelectronic applications.[4] Heat storage by using its MTT with relatively large latent heat is an emerging application, with a hope of better energy utilization.[2]

Attempts were made to synthesize VO_2 by a sol–gel process,[5] pulsed laser deposition[6] or hydrothermal method.[7] Conventionally, however, VO_2 is prepared *via* a thermal reduction route from the most stable V_2O_5, passing through an intermediate state of V_2O_3.[4] A process through such an intermediate state is not always ideal due to subtle dependence on the oxygen partial pressure. There is an alternative of the reduction of metal oxides. Co-milling metal oxides (MO) with hydrocarbon (HC) results in the reduction of MO due to oxidative decomposition of HC with simultaneous oxygen abstraction.[8,9] Such a mechanochemical process is capable to preparing various oxides with lower oxidation number or suboxides.[9] In most cases, HC-based polymers (PHC) like polyethylene or polypropylene were used as a HC source.[9–11] The process is convenient since it is solvent free so that no drying process is necessary and hence environmentally benign. On the other hand, there is also a bottleneck. A significant amount of decomposed polymer remains with various stages of fragmentation. Since they are in most cases insoluble in most of the organic solvents, post heating under controlled atmosphere is necessary when they must be eliminated. Use of non-polymer hydrocarbon (NPHC) is an alternative for the mechanochemical reduction of MO, since they can be easily eliminated by conventional extraction or washing.

The primary objective of the present study is to examine the preparation process of VO_2 *via* mechanochemical reduction by using NPHC. Since one of the main applications of VO_2 is heat storage associated with its latent heat of phase transformation, we used differential scanning calorimetry as a main tool for evaluating its functionality. To close up particularity of the mechanochemical reduction, we observed, aside from usual chemical and structural properties, the electronic states of the product by X-ray photoelectron spectroscopy (XPS) combined with ion-etching procedure and compared them with those of commercially available VO_2.

[a]*Advanced Ceramics Research Center, Nagoya Institute of Technology, Tajimi, Japan. E-mail: senna@applc.keio.ac.jp; fuji@nitech.ac.jp*

[b]*Faculty of Science and Technology, Keio University, Yokohama, Japan*

† Electronic supplementary information (ESI) available. See DOI: 10.1039/c8ra02159g

This journal is © The Royal Society of Chemistry 2018

Open Access Article. Published on 11 June 2018. Downloaded on 1/25/2026 10:46:13 PM.
This article is licensed under a Creative Commons Attribution-NonCommercial 3.0 Unported Licence.

Experimental section

Sample preparation

Commercial V_2O_5 (Kanto Chemical) was mixed with a NPHC, *i.e.* a paraffin wax (PW, C_nH_{2n+2}, n = 18–46, average molecular weight 254–646, melting point 56–58 °C, Kanto Chemical). An aliquot of dispersion containing fixed amount, 2.2 g, of V_2O_5 with varying mass ratio V_2O_5 : PW (MRVP) was put into a milling vessel together with milling balls, 6 pieces of 15 mm plus 6 pieces of 5 mm in diameter. Both the vessel and balls were made of highly sintered yttria-stabilized zirconia. The mass ratio of the sample and the milling ball was fixed at 30 : 1. We also prepared cation doped VO_2 by adding 1 atom% of Cr_2O_3, MoO_3 or WO_3 to V_2O_5 and milled under the same condition.

The mechanochemical treatment was carried out by using a planetary mill (Fritsch Pulverisette 5) in air for varying duration. After milling, the contents were separated from the milling ball and washed twice by *n*-hexane for 30 min and dried at 120 °C under reduced pressure. Commercial VO_2 (Nanowire VO_2, Sigma Aldrich) was used for comparison. We also used a commercial heat storage material, a chrome-doped vanadium dioxide, Smartec HS 70® with a nominal composition $V_{1-x}Cr_xO_2$ (Kojundo Chemical Laboratory Co., Ltd).

Characterization

Crystallographical properties were monitored by conventional X-ray diffractometry with RINT1000, Rigaku Corporation, under 40 kV, 40 mA. Thermal properties were examined by differential scanning calorimeter (DSC, Thermo Plus DSC 8230, Rigaku Corporation). Three heating–cooling cycles were repeated under the rates of heating and cooling at 10 °C min^{-1} under pure air flow. The results were adopted from the third cycle, unless otherwise stated. Oxidation states of vanadium were examined by XPS (PHI 5000, Versa Probe II, Ulvac-Phi, Inc). Ar ion etching was also performed at 1 keV up to 10 min with 1 min interval to examine the difference in the electronic states between the topmost surface and near surface interior. Microstructures were observed by a scanning electron microscope, JSM-7600F, JEOL. Thermal stability of the products was examined by repeated cycles of TG-DTA (Thermo Plus TG8120, Rigaku Corporation) at 10 °C min^{-1} up to 500 °C under pure air flow.

Results and discussions

Morphological observation

We first observed the morphology of representative samples under scanning electron microscope (SEM). As shown in Fig. 1, starting V_2O_5 comprises severely agglomerated submicron units. Commercial VO_2, on the other hand, contains particles with well-developed facets (Fig. 2a), reflecting its high crystallinity. Simultaneously, we observe a nano-wired substructure under higher magnification (Fig. 2b and c). As shown in Fig. 3, milling of V_2O_5 in PW brought about conventional disintegration of the crystalline particles.

Thermal properties and latent heat

Representative DSC profiles are shown in Fig. 4 and 5, where (a) and (b) denote the profiles obtained during heating and cooling, respectively. Typical endothermic and exothermic peaks are recognized during heating and cooling, for all the samples examined. This is very similar to those reported for VO_2.[12] Representative values of the phase transition temperature and the latent heat are summarized in Table 1.

Crystallographical properties

Changes in the X-ray diffractograms by mechanochemical treatment are shown in Fig. 6. By increasing milling time with MRVP fixed at 10 : 1, we observe formation of the VO_2 phase (Fig. 6a). However, its phase purity was not attained even after milling for 10 h. As MRVP was increased under the fixed milling time at 3 h, VO_2 became phase pure when MRVP exceeded 20 : 1 (Fig. 6b). The product colored deep green like the commercial one (see Fig. S1 in ESI†).

Representative values of the phase transition temperature and the latent heat are summarized in Table 1. Increasing MRVP brought about increasing extent of VO_2 phase purity as qualitatively recognizable from the X-ray diffractograms shown in Fig. 6. Note that an increase in MRVP and hence, an increase in the VO_2 phase purity parallels the amount of latent heat, as

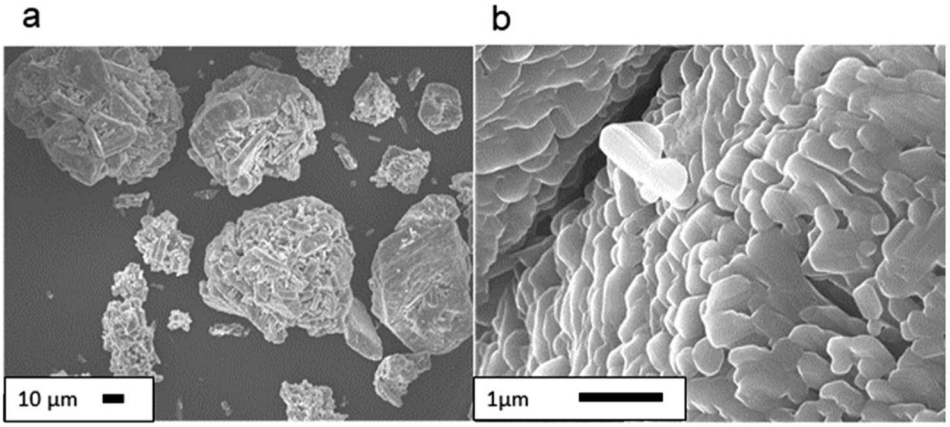

Fig. 1 Scanning electron micrographs of starting V_2O_5 particles.

Open Access Article. Published on 11 June 2018. Downloaded on 1/25/2026 10:46:13 PM.
This article is licensed under a Creative Commons Attribution-NonCommercial 3.0 Unported Licence.

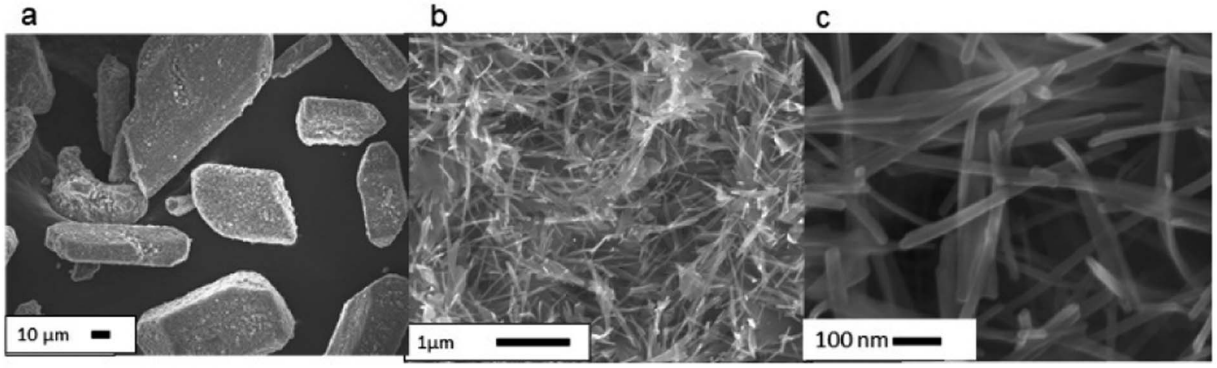

Fig. 2 Scanning electron micrographs of commercial VO_2 particles with varying magnification.

shown in Table 1. The mechanochemically derived sample with MRVP 30 : 1 exhibited its latent heat above 20 J g^{-1}, which was superior over those of the commercial, VO_2.

The difference in the DSC peaks during heating and cooling, *i.e.* thermal hysteresis of the phase change increased with increasing MRVP. It is important to note that this parallels the increase in the latent heat storage capacity. Usually, heat storage capacity increases with increasing crystallinity and associated smaller thermal hysteresis.[13] It is generally understood that the thermal hysteresis reflects the heterogeneity of the material.[12] This counts as an anomalous feature of the present mechanochemically reduced VO_2, as we will discuss below in more detail.

Effects of annealing on the crystallography and heat storage

To examine the role of heterogeneity, we annealed the sample milled for 3 h with MRVP 30 : 1 at 500 °C for 3 h in Ar atmosphere. As shown in Fig. 7, the crystallinity of VO_2 significantly increased after annealing while maintaining its phase purity. The annealed sample showed the peak temperature like those of commercial VO_2. However, the DSC peak broadened, particularly in the exothermic peak during cooling (Fig. 8). More importantly, annealing decreased the latent heat significantly. This suggests that the relatively high latent heat capacity of the present mechanochemically derived VO_2 is associated with the coexistence of high lattice defect concentration, in accordance with the larger thermal hysteresis. Upon annealing the as-milled VO_2, we observed a nano-wired structure (Fig. 9), like those observed in commercial VO_2 (Fig. 2c).

Unique features of mechanochemically prepared VO_2

i Structural properties. As we observed, heat treatment after co-milling of V_2O_5 with PW lead to higher crystallinity with a nano-wired morphology. The related structural analysis has been studied in detail.[14] However, this did not improve the heat

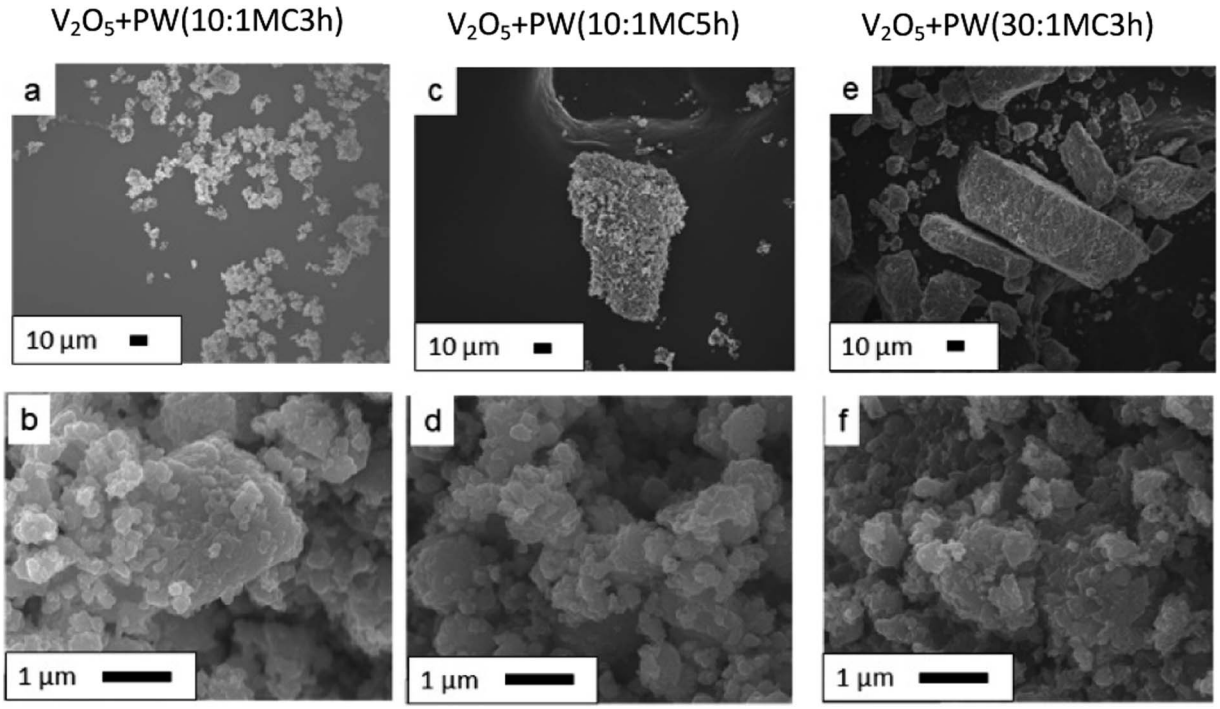

Fig. 3 Change in the particle morphology by milling under different conditions.

This journal is © The Royal Society of Chemistry 2018

Open Access Article. Published on 11 June 2018. Downloaded on 1/25/2026 10:46:13 PM.
This article is licensed under a Creative Commons Attribution-NonCommercial 3.0 Unported Licence.

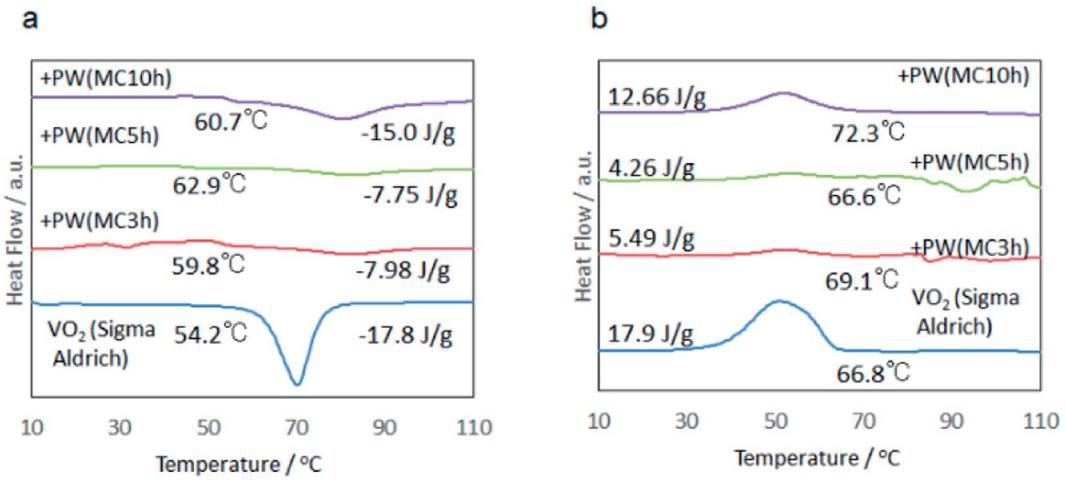

Fig. 4 DSC profiles of the samples for fixed MRVP 10 : 1 with varying milling time. (a) Heating, (b) cooling.

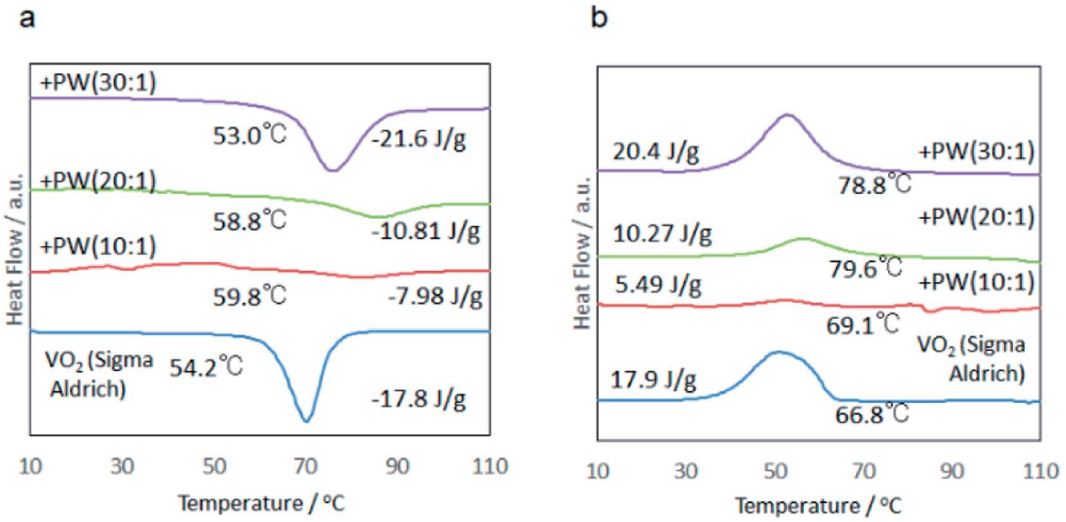

Fig. 5 DSC profiles of the samples for fixed milling time, 3 h, with varying MRVP. (a) Heating, (b) cooling.

storage capacity in our case. Plašienka *et al.* studied by tracing the changes in projected densities of states and their correlation with the evolution of the structural transformation.[15] Their results revealed a strong interconnection between the structural and electronic transformations and show that they take place on the same time scale. Structural and electronic changes of VO_2 were extensively studied from experimental side as well with a well-defined thin film, in conjunction with the lattice mismatch with the substrate.[2,16] Quick concerted action of these two changes is associated with the smaller thermal hysteresis, ΔT_c, and is favorable for many functional properties of VO_2 as well.[17] Therefore, efforts were paid to reduce, ΔT_c.[17,18]

Transition temperature of VO_2 is dominated by many different structural properties. Apart from the effects of doped materials mentioned above, defect structure plays a significant role,[19,20] inducing the further parametrical variables such as the number of heating–cooling cycles.

Mechanochemically derived VO_2 is rich in the strain due to its lattice disturbance particularly in the near surface region.[21] Our results suggested that introduction of near surface lattice strain favors the better heat storage properties. This seems to be incompatible with the previous studies mentioned above. Indeed, mechanochemically treated particles are rich in oxygen vacancies, which increases the low-temperature conductivity of VO_2. This, in turn, is responsible, if partly, for better heat storage.[22] These apparently inconsistent observations should be associated with the particularity of the present VO_2, obtained *via* mechanochemical reduction. In order further to discuss these points, electronic properties were examined below by XPS.

Table 1 Phase transition temperature and amount of latent heat of the samples for fixed milling time, 3 h, with varying V_2O_5 : HC ratio, and commercial VO_2 (Sigma Aldrich)

		+PW (10 : 1)	+PW (20 : 1)	+PW (30 : 1)	VO_2 (Sigma Aldrich)
Transition temp (°C)	Heating	59.8	58.8	53	54.2
	Cooling	69.1	79.6	78.8	66.8
Latent heat ($J\ g^{-1}$)	Heating	−8	−10.8	−21.6	−17.8
	Cooling	5.5	10.3	20.3	17.9

Open Access Article. Published on 11 June 2018. Downloaded on 1/25/2026 10:46:13 PM.
This article is licensed under a Creative Commons Attribution-NonCommercial 3.0 Unported Licence.

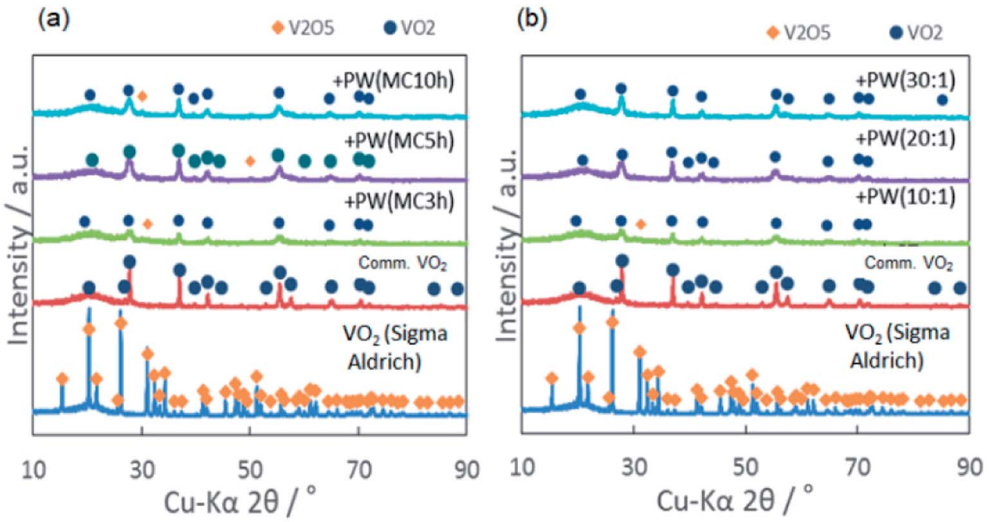

Fig. 6 X-ray diffractograms. (a) For fixed MRVP 10 : 1 with varying milling time, and (b) For fixed milling time, 3 h with varying MRVP.

ii Electronic properties. Mechanochemically derived, defective VO_2 is expected to be different from those prepared in a conventional manner. This was examined by XPS. Fig. 10 and 11 demonstrate V_{2p} XPS peak profiles for representative samples without Ar^+ etching and after 5 min etching, respectively. From Fig. 10, we recognize, first of all, the V^{5+} signal in the $V_{2p3/2}$ peaks at around 517 eV for V_2O_5, in line with the literature value.[23] In spite of the nominal valence state of VO_2, *i.e.* V^{4+}, VO_2 always exhibits the strongest peak just similar to V^{5+} with much smaller peak specific to V^{4+} at around 516 eV.[23] Indeed, the V_{2p} XPS peak profile is different among the commercially available nominal VO_2 samples.[23] We also observed a similar profile from the commercial VO_2 we used, where the letter peak appears on the foot of the asymmetric peak on the low binding energy side. The commercial Cr-doped V_2O_5 with the trade name Smartec 70 exhibits the stronger peak of V^{4+} due to the dopant Cr.

Our mechanochemically derived sample with MRVP 30 : 1 exhibits a unique broad and almost symmetric peak with its summit at around 516.5 eV. This is dissimilar to all the related

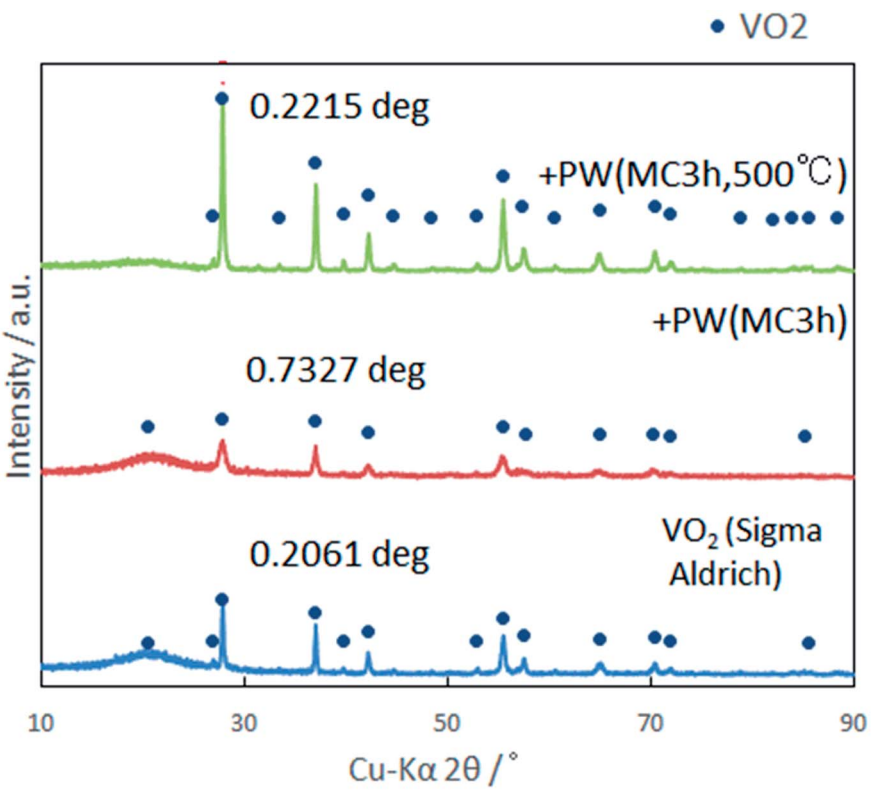

Fig. 7 Effect of annealing based on the X-ray diffractograms compared with the sample before annealing and commercial VO_2.

This journal is © The Royal Society of Chemistry 2018

Open Access Article. Published on 11 June 2018. Downloaded on 1/25/2026 10:46:13 PM.
This article is licensed under a Creative Commons Attribution-NonCommercial 3.0 Unported Licence.

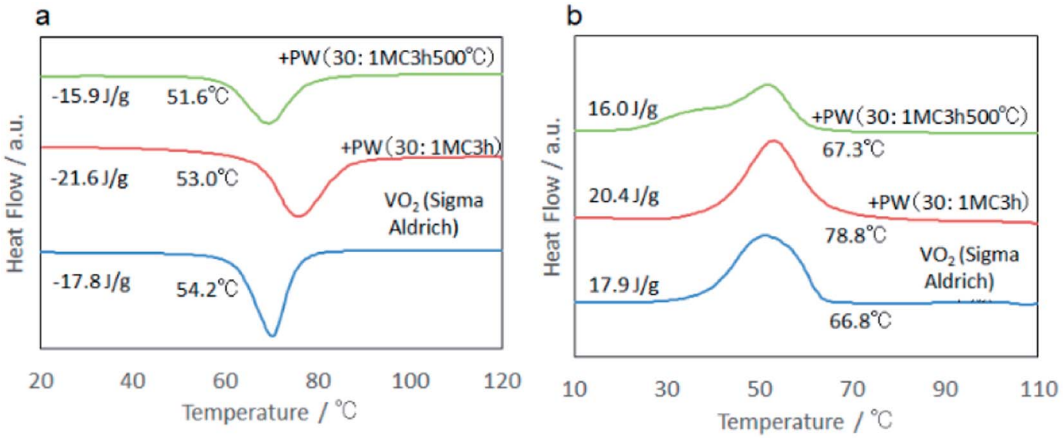

Fig. 8 Effect of annealing based on DSC profiles compared with the sample before annealing and commercial VO_2. (a) Heating, (b) cooling.

samples examined, and hence, demonstrates a unique feature of the oxidation state of vanadium. Broadening and shift of $V_{2p3/2}$ peak toward higher binding energy side upon irradiation of gamma ray were observed by Madiba *et al.*[24] on well-defined VO_2 thin film due to the introduction of structural disorder. They also observed a similar increase in the thermal hysteresis as in our present study. Similar structural degradation was clearly observed in our case, represented by the peak broadening of the X-ray diffractogram, shown in Fig. 6. Broadening of the $V_{2p3/2}$ peak is also associated with the diversity of the cluster size,[25] which is also likely to be the case in the present mechanochemical treatment.

Properties of lattice oxygen in vanadium oxide were extensively studied in the interests of catalytic activity.[26–28] An apparent increase in the intensity at low binding energy side is primarily ascribed to the partial reduction from V^{5+} to V^{4+} as in many similar cases of co-milling transition metal oxides with hydrocarbon species we reported.[9,10] However, there are other components, *i.e.* with structural degradation. It is obvious that significant amount of lattice oxygen atoms of the starting V_2O_5 were abstracted due to fact that VO_2 diffraction peak was predominant from the XRD profiles shown in Fig. 6. Mechanochemical reduction is inevitably associated with the formation of oxygen vacancies, which will be rapidly compensated by the incorporation of gaseous oxygen, which enriches the electron density near vanadium ions, resulting in the peak shift toward the lower binding energy side. This is an additional mechanism of the unique XPS $V_{2p3/2}$ peak shift of sample with MRVP 30 : 1, although this speculative mechanism requires further evidences.

In order further to discuss the electronic states of these 4 representative samples displayed in Fig. 10 and 11, we have Ar-etched all the samples. Change in the $V_{2p3/2}$ XPS profiles with varying etching time for the samples with MRVP 30 : 1 and VO_2 are shown in Fig. S2 and S3,† respectively. We compared their V_{2p} XPS profiles after etching for 5 min in Fig. 11. All three commercial vanadium oxides showed remarkable broadening of the $V_{2p3/2}$ peak toward low binding energy. For the VO_2 based materials, the broadening may simply be interpreted by the elimination of overoxidized near surface region. However, this cannot be the case for V_2O_5. Apparent reduction of metal oxides due to ion etching is generally recognized due to the mass difference between the lighter O^{2-} ions and heavier metal cationic species.[29] Therefore, we attribute the peak broadening by Ar-etching to the combination of both mechanisms mentioned above. The sample with MRVP 30 : 1 showed much smaller change in the $V_{2p3/2}$ peak profile by Ar etching.

From the observations given in this sub-section, we may safely conclude that the mechanochemical reduction of V_2O_5 brings about particles substantially different from any other vanadium suboxides. We also emphasize that the sample with MRVP 30 : 1 exhibits phase transition and associated latent heat. Together with the observed high thermal hysteresis detected by DSC and a unique broad one-peak of $V_{2p3/2}$, the product is heterogeneous but with their electronic states varies within a mass of entire particles with continuous distribution of their electronic states.

iii Thermal stability. Fig. 12 exhibits the thermal stability of the mechanochemically derived product, *i.e.* milled for 3 h with MRVP 30 : 1, examined by TG-DTA in air. They comprise the profiles of first and second cycles for the temperature spans, 50–200 °C (Fig. 12a and b) and 50–500 °C (Fig. 12c and d). The TG and DTA profiles of the first and second cycle profiles up to 200 °C are similar. However, a gradual weight loss was observed

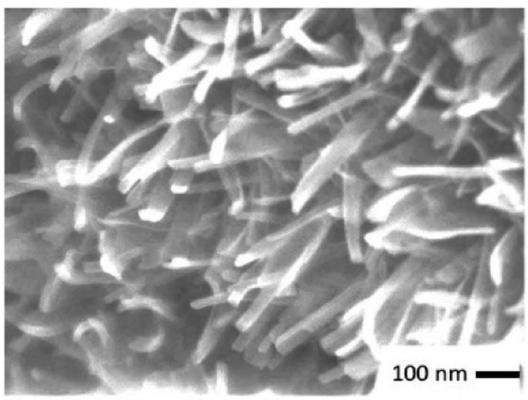

Fig. 9 Scanning electron micrograph of the sample V_2O_5 + PW(MC3h) after annealing at 500 °C for 3 h.

Open Access Article. Published on 11 June 2018. Downloaded on 1/25/2026 10:46:13 PM.
This article is licensed under a Creative Commons Attribution-NonCommercial 3.0 Unported Licence.

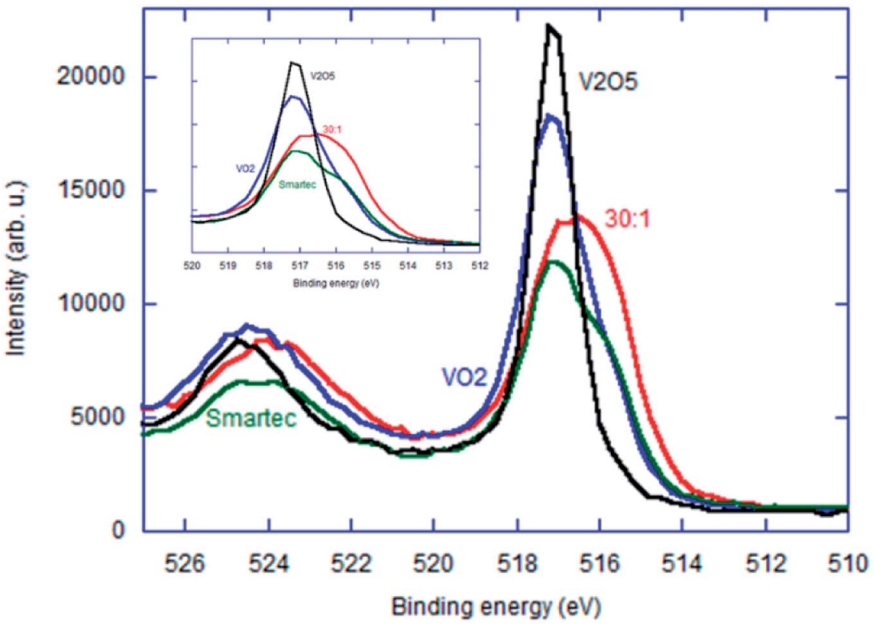

Fig. 10 V_{2p} XPS profiles of topmost surface without ion etching.

only at the first cycle, in an amount to 3.6 wt% by heating up to 200 °C. Commercial VO_2 exhibited similar thermal behavior as shown in Fig. S4.† The total weight loss was less than 2 mass%, *viz.* smaller than that of the mechanochemically derived VO_2. While the latter weight loss is attributable to the dehydration of sorbed water during storage, the rest of the weight loss, *i.e. ca.* 1.8 wt% must be due the sources different from sorbed water. We suspect the extra weight loss due to the rest of PW, despite careful washing by *n*-hexane and subsequent drying. This will be further discussed below.

Since the position and integral intensity of the endothermic peak due to the phase change remained almost unchanged, we may adopt that the present mechanochemically derived VO_2 is stable up to 200 °C in air for heat storage. At temperatures above 300 °C, significant weight loss up to 8 mass% was observed (Fig. 12c). This was accompanied by a very broad exothermic peak at around 400 °C. The reason for the weight loss cannot be explained by oxidation. Rather, the apparent heat loss might be associated with a kind of dehydroxylation of firmly hydrated OH groups[18] on the surface during wet milling.

iv Comparison with commercial heat storage material based on VO_2. The commercially available heat storage material, Smartec HS 70, is based on the chromium-doped V_2O_5. It possesses a high crystallinity (Fig. S5†) and exhibits the latent

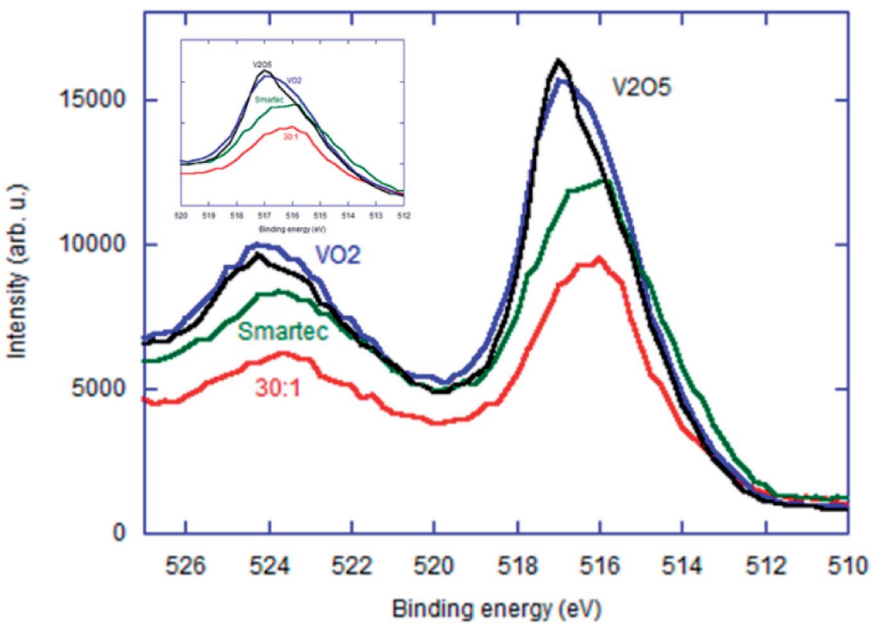

Fig. 11 V_{2p} XPS profiles of topmost surface after A^+ ion etching for 5 min.

This journal is © The Royal Society of Chemistry 2018

Open Access Article. Published on 11 June 2018. Downloaded on 1/25/2026 10:46:13 PM.
This article is licensed under a Creative Commons Attribution-NonCommercial 3.0 Unported Licence.

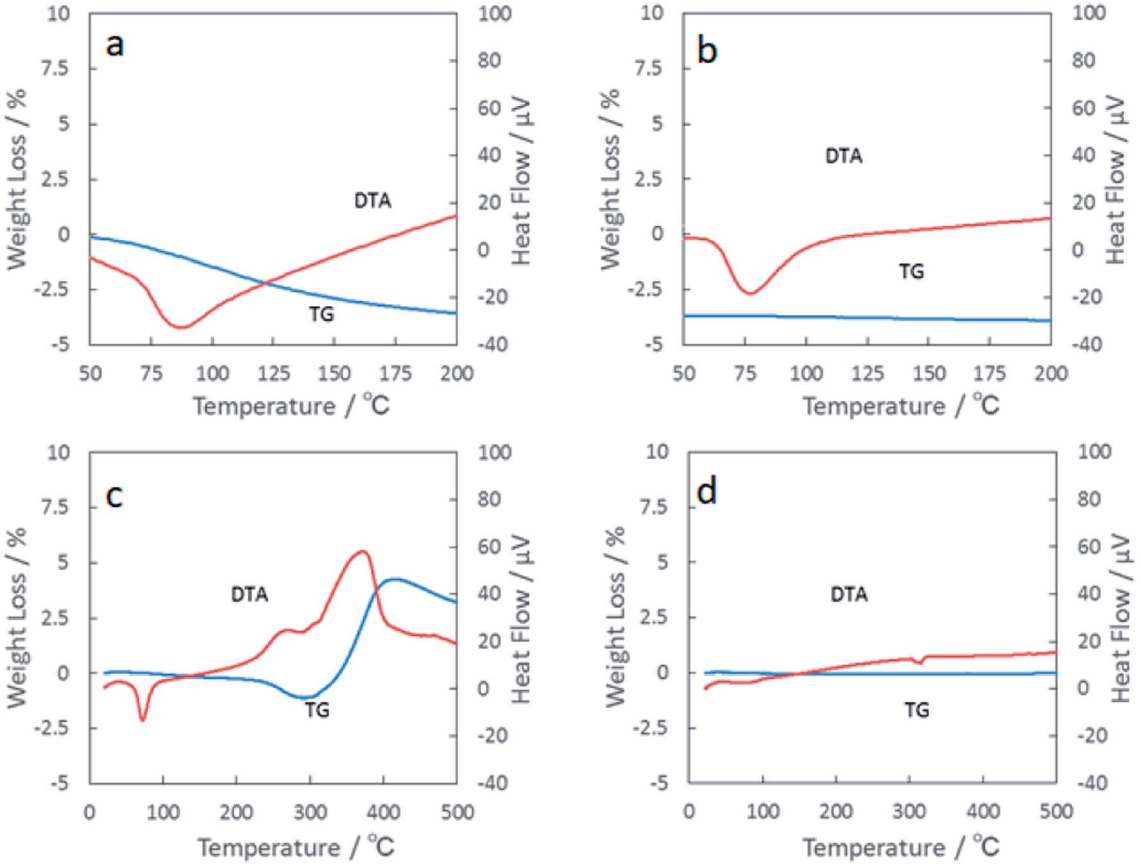

Fig. 12 TG-DTA profiles of the first and second cycles for the temperature spans, 50 °C–200 °C (a and b) and 50 °C–500 °C (c and d).

heat, −38.78 and 37.19 J g^{-1} during heating and cooling, respectively (Fig. S6†). They are almost twice as large as our VO_2. It is documented that doping of Cr and/or Nb to VO_2 changes the thermal hysteresis and the temperature coefficient of the resistance toward favorable latent heat capacitance.[30]

Therefore, we examined the effects of cation doping. As shown in Fig. 13, doping of all the cationic species examined, *i.e.* Cr, Mo and W, brought about a decrease in the latent heat. Shift of the transition temperature compared with the commercial VO_2 was also smaller than those obtained by milling without doping. Although we do not have enough evidences for these phenomena, these results also indicate the difference in the transition temperature and the amount of latent heat from VO_2 prepared in a conventional manner.

v **Possible role of remaining PW.** From the difference in the weight loss between those from the mechanochemically derived and commercial one, persistence of PW up to 1.8 wt% was suspected even after carefully washed by *n*-hexane and dried,

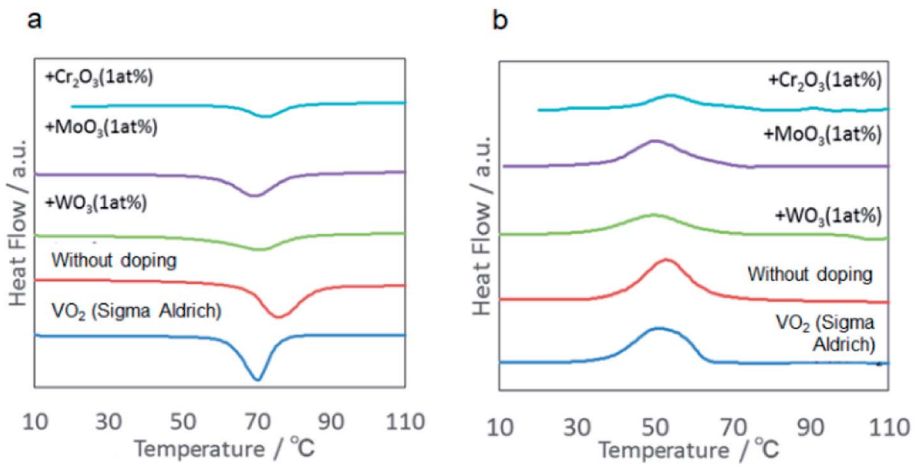

Fig. 13 Effect of cation doping to the sample obtained after milling at MRVP 30 : 1 for 3 h on DSC profiles. (a) Heating, (b) cooling.

Open Access Article. Published on 11 June 2018. Downloaded on 1/25/2026 10:46:13 PM.
This article is licensed under a Creative Commons Attribution-NonCommercial 3.0 Unported Licence.

due to possible chemical adsorption. Interaction between vanadium oxides and hydrogen and hydrocarbon has been extensively studied in the interests of their catalytic activity.[31,32] On the surface of transition metal oxides, there are electron donor and acceptor sites simultaneously. These feature is generally enhanced by the mechanical activation by introducing various lattice defects.[21] Remaining PW could also contribute to the enhanced heat storage, since they are also applied to phase change thermal energy storage,[33,34] with their latent heat up to ten times higher than usual VO_2.[35]

Conclusions

Mechanochemically derived phase pure VO_2 obtained by milling V_2O_5 in a paraffin wax (PW) with the mass ratio V_2O_5 : PW 30 : 1 exhibits its latent heat above 20 J g^{-1}, which is higher than that of commercial VO_2. Neither cation doping nor post annealing increased the latent heat capacity. The thermal hysteresis increased with increasing mass ratio. These unique properties of mechanochemically derived VO_2 is primarily ascribed to the abundance of V^{4+} ionic states stabilized by simultaneously introduced structural degradation throughout the entire particles as we confirmed by X-ray photoelectron spectroscopy in terms of $V_{2p3/2}$ peaks combined with Ar^+ ion etching. Remaining PW up to 1.8 wt% may have also contributed to the additional increase in the heat storage capacity.

Conflicts of interest

There are no conflicts to declare.

Acknowledgements

This study was supported by JSPS KAKENHI Grant Number 17J40042 and JST Adaptable and Seamless Technology transfer Program through target-driven R&D (JST A-STEP). This research is partially supported by "Knowledge Hub Aichi", Priority Research Project from Aichi Prefectural Government.

References

1 M. Telkes, The Efficiency of Thermoelectric Generators. I, *J. Appl. Phys.*, 1947, **18**, 1116–1127.
2 L. Long, H. Ye, Y. Gao and R. Zou, Performance Demonstration and Evaluation of the Synergetic Application of Vanadium Dioxide Glazing and Phase Change Material in Passive Buildings, *Appl. Energy*, 2014, **136**, 89–97.
3 F. J. Morin, Oxides Which Show a Metal-to-Insulator Transition at the Neel Temperature, *Phys. Rev. Lett.*, 1959, **3**, 34–36.
4 S. G. Corr, M. Grossman, J. D. Furman, B. C. Melot, A. K. Cheetham, K. R. Heier and R. Seshadri, Controlled Reduction of Vanadium Oxide Nanoscrolls, *Chem. Mater.*, 2008, **20**, 6396–6404.
5 N. Wang, S. Liu, X. T. Zeng, S. Magdassi and Y. Long, Mg/W-Codoped Vanadium Dioxide Thin Films with Enhanced Visible Transmittance and Low Phase Transition Temperature, *J. Mater. Chem. C*, 2015, **3**, 6771–6777.
6 R. McGee, A. Goswami, B. Khorshidi, K. McGuire, K. Schofield and T. Thundat, Effect of Process Parameters on Phase Stability and Metal-Insulator Transition of Vanadium Dioxide (VO_2) Thin Films by Pulsed Laser Deposition, *Acta Mater.*, 2017, **137**, 12–21.
7 K. Ran, W. Huang, Q. Shi, L. Tang, B. Peng, S. Liang, H. Zhu and Z. Mao, Freeze-Drying Induced Nanocrystallization of VO_2 (M) with Improved Mid-Infrared Switching Properties, *J. Alloys Compd.*, 2017, **728**, 1076–1082.
8 W. K. Choi, J. S. Cho, S. K. Song, H. J. Jung, S. K. Koh, K. H. Yoon, C. M. Lee, M. C. Sung and K. Jeong, The Characterization of Undoped Snox Thin Film Grown by Reactive Ion-Assisted Deposition, *Thin Solid Films*, 1997, **304**, 85–97.
9 M. Senna, *et al.,* Fluorine Incorporation into Sno2 Nanoparticles by Co-Milling with Polyvinylidene Fluoride, *Solid State Sci.*, 2014, **30**, 36–43.
10 M. Senna, V. Šepelák, J. Shi, B. Bauer, A. Feldhoff, V. Laporte and K.-D. Becker, Introduction of Oxygen Vacancies and Fluorine into TiO_2 Nanoparticles by Co-Milling with Ptfe, *J. Solid State Chem.*, 2012, **187**, 51–57.
11 M. Senna, N. Myers, A. Aimable, V. Laporte, C. Pulgarin, O. Baghriche and P. Bowen, Modification of Titania Nanoparticles for Photocatalytic Antibacterial Activity Via a Colloidal Route with Glycine and Subsequent Annealing, *J. Mater. Res.*, 2012, **28**, 354–361.
12 G. A. Horrocks, S. Singh, M. F. Likely, G. Sambandamurthy and S. Banerjee, Scalable Hydrothermal Synthesis of Free-Standing VO(2) Nanowires in the M1 Phase, *ACS Appl. Mater. Interfaces*, 2014, **6**, 15726–15732.
13 M. Li, S. Magdassi, Y. Gao and Y. Long, Hydrothermal Synthesis of VO_2 Polymorphs: Advantages, Challenges and Prospects for the Application of Energy Efficient Smart Windows, *Small*, 2017, **13**, 1701147.
14 Y. R. Jo, S. H. Myeong and B. J. Kim, Role of Annealing Temperature on the Sol–Gel Synthesis of VO_2 Nanowires with in Situ Characterization of Their Metal–Insulator Transition, *RSC Adv.*, 2018, **8**, 5158–5165.
15 D. Plašienka, R. Martoňák and M. C. Newton, Ab Initio Molecular Dynamics Study of the Structural and Electronic Transition in VO_2, *Phys. Rev. B*, 2017, **96**, 0541110.
16 X. He, N. Punpongjareorn, W. Liang, Y. Lin, C. Chen, A. J. Jacobson and D. S. Yang, Photoinduced Strain Release and Phase Transition Dynamics of Solid-Supported Ultrathin Vanadium Dioxide, *Sci. Rep.*, 2017, **7**, 10045.
17 X. Li, L. Yang, S. Zhang, X. Li, J. Chen and C. Huang, VO_2 (M) with Narrow Hysteresis Width from a New Metastable Phase of Crystallized VO_2 (M) $0.25H_2O$, *Mater. Lett.*, 2018, **211**, 308–311.
18 X. Li, S. Zhang, L. Yang, X. Li, J. Chen and C. Huang, A Convenient Way to Reduce the Hysteresis Width of VO_2(M) Nanomaterials, *New J. Chem.*, 2017, **41**, 15260–15267.
19 M. Li, X. Wu, L. Li, Y. Wang, D. Li, J. Pan, S. Li, L. Sun and G. Li, Defect-Mediated Phase Transition Temperature of VO_2 (M) Nanoparticles with Excellent Thermochromic

 This journal is © The Royal Society of Chemistry 2018

Open Access Article. Published on 11 June 2018. Downloaded on 1/25/2026 10:46:13 PM.
This article is licensed under a Creative Commons Attribution-NonCommercial 3.0 Unported Licence.

Performance and Low Threshold Voltage, *J. Mater. Chem. A*, 2014, **2**, 4520–4523.

20 W. Li, S. Ji, Y. Li, A. Huang, H. Luo and P. Jin, Synthesis of VO_2 Nanoparticles by a Hydrothermal-Assisted Homogeneous Precipitation Approach for Thermochromic Applications, *RSC Adv.*, 2014, **4**, 13026–13033.

21 M. Senna, How Can We Make Solids More Reactive? Basics of Mechanochemistry and Recent New Insights, *ChemTexts*, 2017, **3**, 4–13.

22 J. Zhang, Z. Zhao, J. Li, H. Jin, F. Rehman, P. Chen, Y. Jiang, C. Chen, M. Cao and Y. Zhao, Evolution of Structural and Electrical Properties of Oxygen-Deficient VO_2 under Low Temperature Heating Process, *ACS Appl. Mater. Interfaces*, 2017, **9**, 27135–27141.

23 G. Silversmit, D. Depla, H. Poelman, G. B. Marin and R. De Gryse, Determination of the V_{2p} Xps Binding Energies for Different Vanadium Oxidation States (V^{5+} to V^{0+}), *J. Electron Spectrosc. Relat. Phenom.*, 2004, **135**, 167–175.

24 I. G. Madiba, N. Émond, M. Chaker, F. T. Thema, S. I. Tadadjeu, U. Muller, P. Zolliker, A. Braun, L. Kotsedi and M. Maaza, Effects of Gamma Irradiations on Reactive Pulsed Laser Deposited Vanadium Dioxide Thin Films, *Appl. Surf. Sci.*, 2017, **411**, 271–278.

25 C. Hess, G. Tzolova-Müller and R. Herbert, The Influence of Water on the Dispersion of Vanadia Supported on Silica Sba-15: A Combined Xps and Raman Study, *J. Phys. Chem. C*, 2007, **111**, 9471–9479.

26 A. Bande and A. Lüchow, Vanadium Oxide Compounds with Quantum Monte Carlo, *Phys. Chem. Chem. Phys.*, 2008, **10**, 3371–3376.

27 S. Sugiyama, T. Hashimoto, Y. Tanabe, N. Shigemoto and H. Hayashi, Effects of the Enhancement of the Abstraction of Lattice Oxygen from Magnesium Vanadates Incorporated with Copper(II) Cations on the Oxidative Dehydrogenation of Propane, *J. Mol. Catal. A: Chem.*, 2005, **227**, 255–261.

28 K. Fukudome, N.-o. Ikenaga, T. Miyake and T. Suzuki, Oxidative Dehydrogenation of Propane Using Lattice Oxygen of Vanadium Oxides on Silica, *Catal. Sci. Technol.*, 2011, **1**, 987.

29 H. Li, Y. Muraki, K. Karahashi and S. Hamaguchi, Suboxide/Subnitride Formation on Ta Masks During Magnetic Material Etching by Reactive Plasmas, *J. Vac. Sci. Technol., A*, 2015, **33**, 040602.

30 K. Miyazaki, K. Shibuya, M. Suzuki, K. Sakai, J.-i. Fujita and A. Sawa, Chromium–Niobium Co-Doped Vanadium Dioxide Films: Large Temperature Coefficient of Resistance and Practically No Thermal Hysteresis of the Metal–Insulator Transition, *AIP Adv.*, 2016, **6**, 055012.

31 M. Witko, K. Hermann and R. Tokarz, Ab Initio and Semiempirical Cluster Studies on the Reactivity of the Vanadium Pentoxide (010), *J. Electron Spectrosc. Relat. Phenom.*, 1994, **69**, 89–98.

32 M. Witko and K. Hermann, Hydrogen Adsorption and Oh Desorption at Vanadium Pentoxide Surfaces: Ab Initio Cluster Model Studies, *J. Mol. Catal.*, 1993, **81**, 279–292.

33 M. K. Rathod and J. Banerjee, Experimental Investigations on Latent Heat Storage Unit Using Paraffin Wax as Phase Change Material, *Exp. Heat Transfer*, 2013, **27**, 40–55.

34 J. Yang, L. Yang, C. Xu and X. Du, Experimental Study on Enhancement of Thermal Energy Storage with Phase-Change Material, *Appl. Energy*, 2016, **169**, 164–176.

35 J. Kurdi, S. Al-Muhtaseb, B. Madadkhahsalmassi and M. Farid, Screening Alternatives for Producing Paraffinic Phase Change Materials for Thermal Energy Storage in Buildings, *Int. J. Energy Res.*, 2017, **41**, 1932–1940.